Supporting Information

1. Methods

1.1. Synthesis and characterization of polymers

The homopolymer PDL and copolymer mPEG-b-PDL were synthesized using benzyl alcohol and $mPEG_{5k}$ as initiator according to the reported procedure. The synthesis and purification of polymers were confirmed by ^{1}HNMR values [1].

1.2. *Ex vivo* permeation study

Fresh pig ear skin was collected from a local slaughterhouse. The skin was thoroughly washed with a buffer solution, the hair on it was removed with a surgical razor, the skin was separated from the underlying cartilage, and subcutaneous fat was removed with a scalpel [2]. Franz diffusion cell with an effective diffusion area of 3.14 cm^2 was utilized to conduct the *ex vivo* permeation study. The previously prepared skin was clamped between the donor and receptor chambers of the diffusion cell. The receptor chamber was filled with freshly prepared 10% methanol-added phosphate buffer (pH 5.5). The receptor diffusion cell was maintained at 37°C and a stirring rate of 200 rpm. The coarse KTZ-EUG-Gel and KTZ-EUG-NE-Gel were applied to the skin. A 1 ml sample at 0.5, 1, 2, 4, 8, and 12h time intervals was collected and replenished with the same amount to maintain sink conditions. The sample was filtered and analyzed using the validated RP-HPLC method. The experiment was performed in triplicate (n = 3), and data were plotted for the cumulative amount of drug permeated against time [3].

The values obtained from coarse-KTZ-EUG-Gel and KTZ-EUG-NE-Gel were compared using the steady-state transdermal flux (Jss) and permeability coefficient (Kp), which were calculated using **Eq. 1**. When plotting the cumulative amount of drug permeated (cm^{-2}) against time, Jss was found from the linear slope of the line. Using a flux to the drug concentration at the donor compartment (Co), Kp was calculated as follows:

$$Jss = \frac{dQ}{dt.A} \quad \textbf{(1)}$$

$$Kp = Jss/Co \quad \textbf{(2)}$$

1.3. Skin retention study

When the *ex vivo* permeation study was completed, the skin was taken out of the Franz diffusion cell. The non-permeated amount of gel was removed with a cotton swab and rinsed

with phosphate buffer saline (PBS) of pH 7.4. The tape-stripping method was utilized to investigate the drug retention at different superficial layers of the skin. The stratum corneum was removed using twelve tape strips. The dermis and epidermis were removed in the same manner and cut into pieces. The drug was extracted from the stripes and skin using methanol. The solution containing drugs was centrifuged, and the supernatant solution was filtered and analyzed using the developed RP-HPLC method [4].

In addition, the permeation or retention of KTZ or EUG was conducted after the preparation of fluorescent-loaded NE-Gel. The FITC was taken as a contrasting agent owing to lipophilic properties, mimicking KTZ and EUG. Thus, the permeation of FITC can be correlated to the *ex vivo* permeation of KTZ and EUG. In the previous *ex vivo* quantitative permeation study, the higher drug concentration was permeated after 12h. Thus, the fluorescent images of the skin were taken after 12h to investigate the FITC-NE-Gel permeation or retention. After the successful 12h permeation, the skin was removed, and processing was carried out as mentioned by Chwiej et al [5]. A 10µm section of skin was cut using a microtome (HistoCore Multicut, Leica). The section of skin was analyzed for permeation or retention of FITC using a fluorescence microscope (Invitrogen, ThermoFisher Scientific) under suitable magnification. The images were taken in brightfield and fluorescent view mode to determine the presence of FITC in the skin layers.

1.4. *In vitro* antifungal studies

1.4.1. Disk diffusion assay (DDA)

DDA was conducted on yeast extract peptone dextrose agar plates. Briefly, the fungal strain ATCC 90028 was incubated on YPD medium and grown overnight at 30°C with agitation at 100 rpm. The cells were further pelleted, washed, and examined using a hemocytometer for cell count, followed by dilution with YPD agar medium. A 20µl of 1×10^7 *C. albicans* cells were transferred to YPD agar and transferred to 100-mm-diameter Petri dishes. The 10µlof each coarse KTZ-EUG dispersion, Blank NE, and KTZ-EUG-NE were spared on YPD plates and incubated at 30° C [4, 6, 7]. After 24h of incubation, the plates were analyzed for the zone of inhibition.

1.4.2. Effect of the formulations on planktonic growth

The protocol employed to conduct planktonic growth strictly adhered to Clinical Laboratory Standards Institute (CLSI) guidelines. *C. albicans* cells (1×10^3 cells/mL) containing ten different concentrations of coarse KTZ-EUG dispersion, blank NE, and KTZ-EUG-NE (3,1.25,

0.625,0.312,0.156,0.078,0.039 and 0.019 µg/ml) were prepared in RPMI-1640. The well without drugs or formulations was treated as the control group. Concentrations containing 100 µl of *C. albicans* cells and 100 µl of coarse KTZ-EUG dispersion, blank NE, and KTZ-EUG-NE were added to a 96-well microtiter plate. The plate was incubated at 35^{o}C for 48h and was analyzed by measuring the optical density at 620 nm using a microplate reader (Multiskan sky spectrophotometer). The concentration at which 50% growth was reduced was considered MIC_{50} for planktonic growth [4, 7, 8]. The entire experiment was carried out in triplicates, and data were represented as mean ±SD.

1.4.3. Effect of formulations on yeast to hyphal morphogenesis (Y-H Morphogenesis)

The effect of formulations on yeast to hyphal morphogenesis in *C. albicans* was studied using fetal bovine serum (FBS). The concentration range of coarse KTZ-EUG dispersion, blank NE, and KTZ-EUG-NE (3,1.25, 0.625,0.312,0.156,0.078,0.039 and 0.019 µg/ml) was prepared in 20% FBS, and cells without treatment were considered as controls. The plates containing 1×10^{6} cells/ml cells were incubated at 37℃, with 100 rpm shaking for 90 min. The percentage of yeast and hyphal forms in each well was counted, and the concentration at which 50% yeast to hyphal formation was considered as MIC_{50} for yeast to hyphal morphogenesis [4, 7, 8]. The experiment was performed in triplicate.

1.4.4. Effect of the formulation on Candida albicans biofilm formation

To check the KTZ-EUG-NE activity against biofilm development, cells were allowed to adhere to the polystyrene surface of 96 well-treated plates for 90 min. The incubated wells were washed with sterile PBS and RPMI 1640 medium comprising coarse KTZ-EUG dispersion, blank NE, and KTZ-EUG-NE at different concentrations (3, 1.25, 0.625, 0.312, 0.156, 0.078, 0.039 and 0.019 µg/ml) was added to each well. The plate was incubated for 48h at 37°C, and biofilm growth was observed under an inverted microscope and quantified using the XTT metabolic assay [4, 7, 8].

2. Supplementary figures

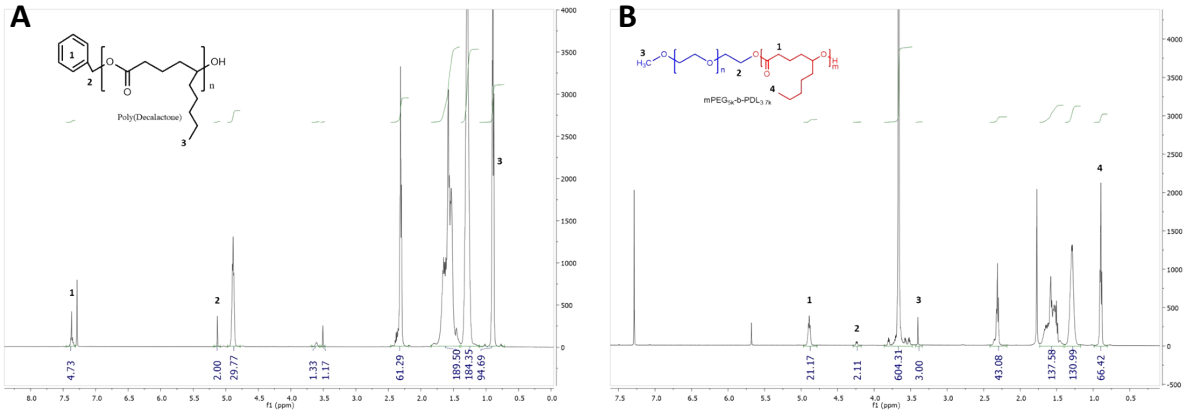

Figure S1 ^{1}HNMR spectra of **A.** PDL and **B.** mPEG-b-PDL in $CDCl_3$ acquired on Bruker's 500MHz.

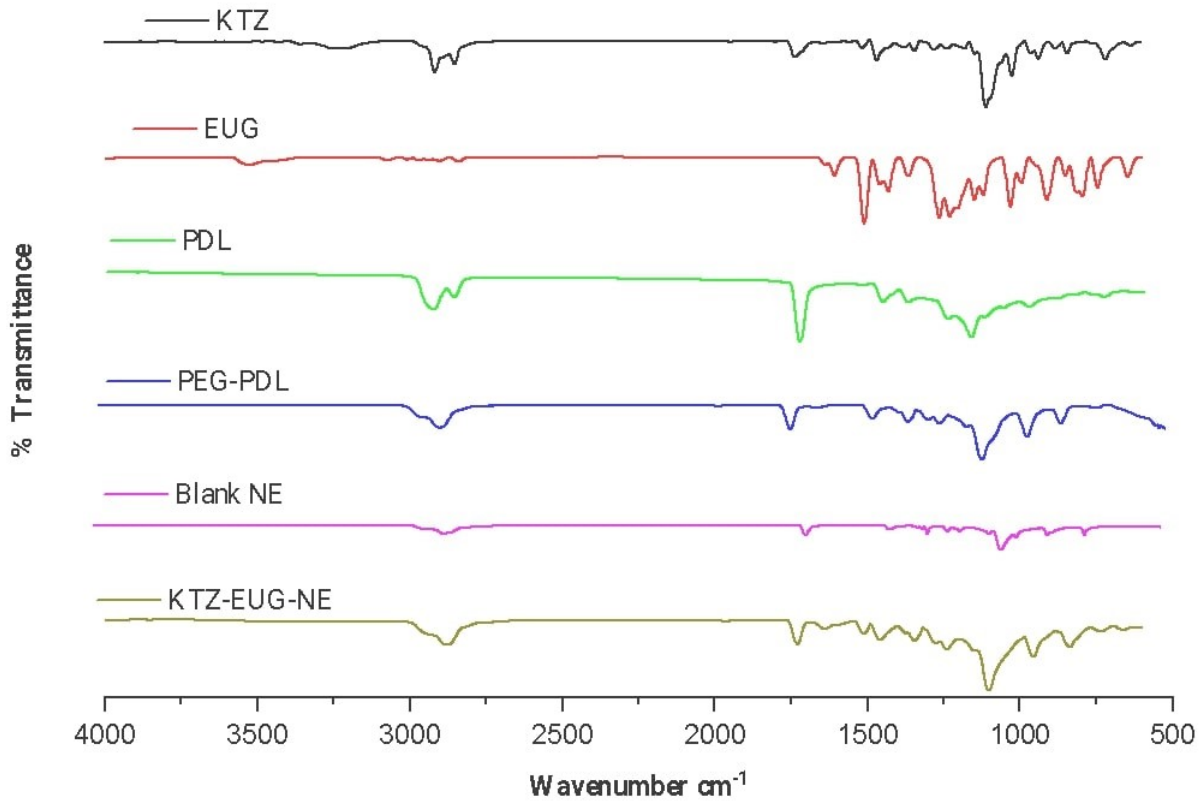

Figure S2 ATR spectrum of KTZ, EUG, PDL, mPEG-b-PDL, Blank NE and KTZ-EUG-NE.

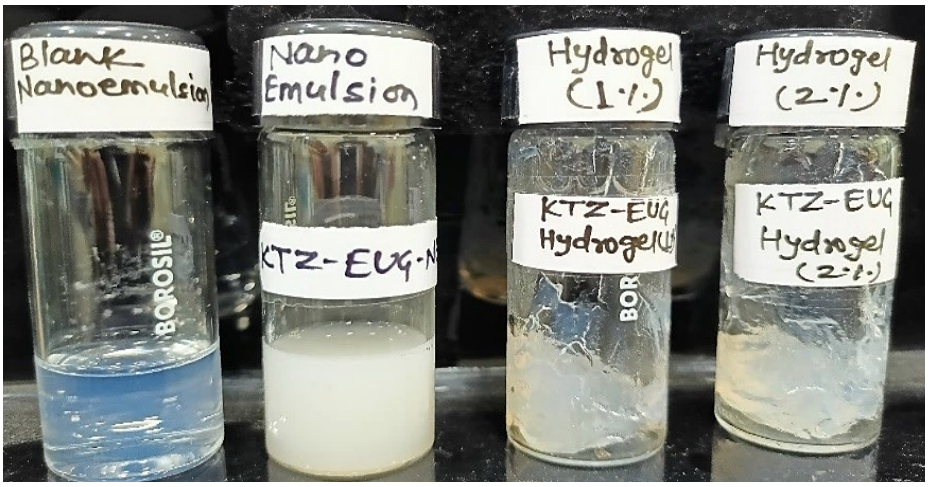

Figure S3 Visual examination of blank NE, KTZ-EUG-NE, 1% KTZ-EUG-NE-Gel and 2% KTZ-EUG-NE-gel.

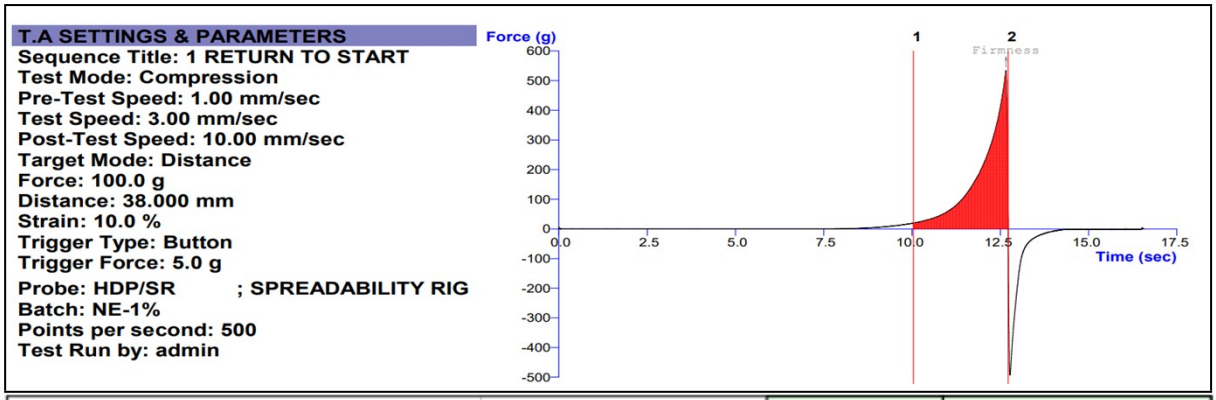

Test ID	Batch	Firmness g Firmness	Work of shear g.sec (Traditional) F-T
Start Batch NE-1%	NE-1%		
NE-1%5	NE-1%	534.675	399.379
End Batch NE-1%	NE-1%		

Figure S4 Spreadability of the 1% KTZ-EUG-NE-Gel tested through texture analyzer (TA-XT plus).

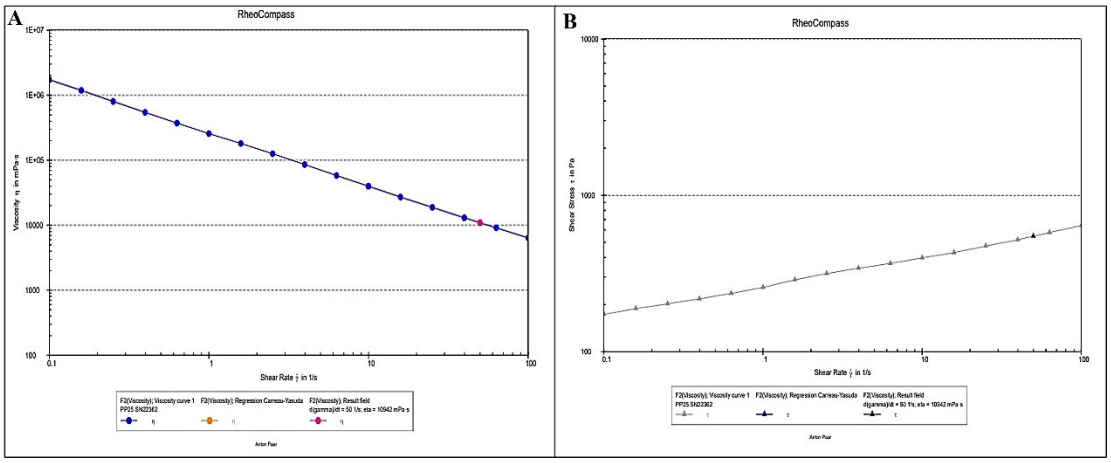

Figure S5 Rheological behavior of optimized 1% w/w KTZ-EU-based NE hydrogel illustrating the correlation of shear rate versus **A.** viscosity **B.** Shear stress.

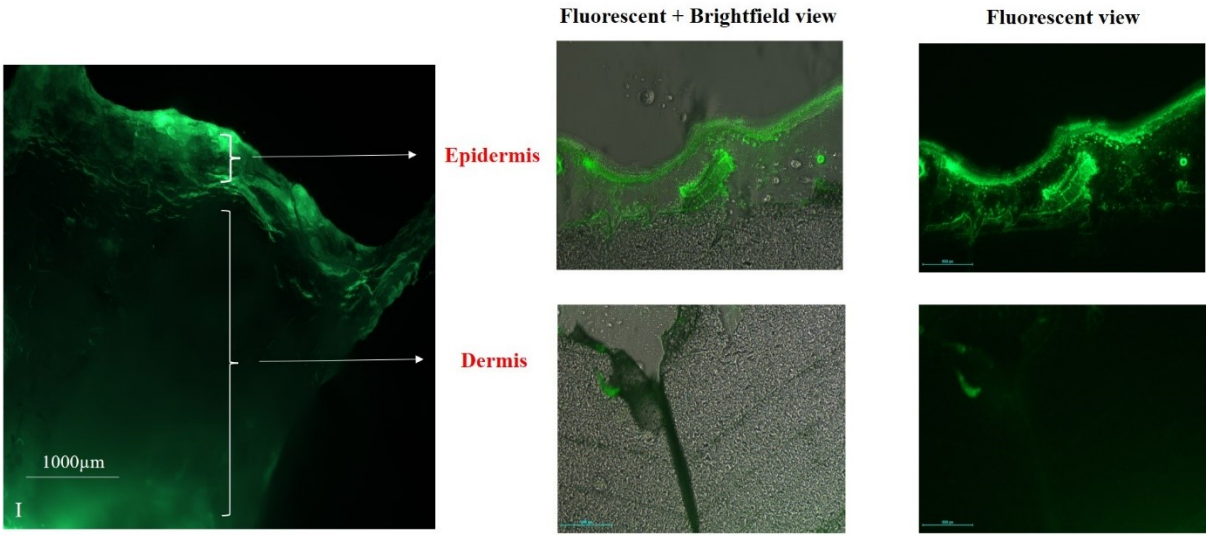

Figure S6 *Ex vivo* permeation study after 12h illustrating I. The retention of FITC-NE-Gel in different layers of the skin, i.e., epidermis and dermis. The brightfield and fluorescent views represent the merged microscopic, focused section, while the green-fluorescent view represents the FITC-NE-Gel.

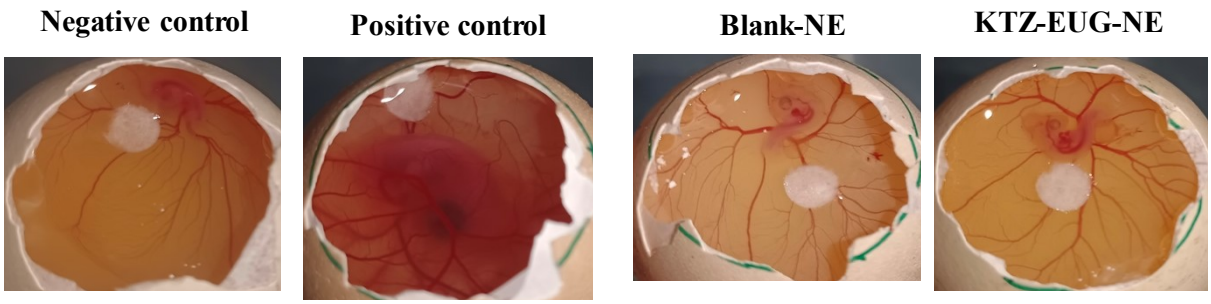

Figure S7 Illustrates the effect of negative control (0.9% NaCl), positive control (300 µL of 0.1M NaOH), Blank NE, and KTZ-EUG-NE after treatment.

3. Supplementary tables

Table S1. QTPP parameters concerning KTZ-EUG-NE

Quality target product profile (QTPP)		
Target Product Profile	**Target**	**Justification**
Dosage form	KTZ-EUG-NE	For stability, faster-sustained release effect, and enhanced permeation
Route of administration	Topical when incorporated into the gelling system	To provide a better-localized effect, reduced systemic absorption
Dose strength	0.1% w/w KTZ 0.05% w/v	Dose within the minimum effective concentration range
Appearance	Transparent	Free from grittiness, odor, or color, patient compliance
Globule size	< 200 nm	The lower globule size, enhance permeation from the stratum corneum
Drug content	Maximum	To enhance the efficacy
Release	Sustained release of drugs	Better drug release from the NE within the skin

Table S2. ANOVA table for the estimated globule size with CCD

Source	Sum of Squares	df	Mean Square	*F*-value	*p*-value	
Model	54077.64	9	6008.63	54.53	<0.0001	Significant
A-Surfactant	538.93	1	538.93	4.89	0.0514	
B-Amplitude	3578.45	1	3578.45	32.47	0.0002	
C-Drug	9742.27	1	9742.27	88.41	<0.0001	
AB	1705.28	1	1705.28	15.47	0.0028	
AC	1123.38	1	1123.38	10.19	0.0096	
BC	6105.13	1	6105.13	55.40	<0.0001	
A2	11030.74	1	11030.74	100.10	<0.0001	
B2	18304.24	1	18304.24	166.10	<0.0001	
C2	7785.73	1	7785.73	70.65	<0.0001	
Residual	1101.99	10	110.20			
Lack of Fit	904.72	5	180.94	4.59	0.0600	Not significant
Pure Error	197.28	5	39.46			
Cor Total	55179.63	19				

Table S3. ANOVA table for the estimate PDI with CCD

Source	Sum of Squares	df	Mean Square	*F*-value	*p*-value	
Model	0.2182	9	0.0242	34.89	< 0.0001	significant
A-Surfactant	0.0002	1	0.0002	0.2531	0.6258	
B-Amplitude	0.0156	1	0.0156	22.41	0.0008	
C-Drug	0.0808	1	0.0808	116.32	< 0.0001	
AB	0.0003	1	0.0003	0.4680	0.5094	
AC	0.0096	1	0.0096	13.81	0.0040	
BC	0.0028	1	0.0028	3.99	0.0735	
A^2	0.0291	1	0.0291	41.92	< 0.0001	
B^2	0.0122	1	0.0122	17.50	0.0019	
C^2	0.0838	1	0.0838	120.59	< 0.0001	
Residual	0.0069	10	0.0007			
Lack of Fit	0.0053	5	0.0011	3.34	0.1058	not significant
Pure Error	0.0016	5	0.0003			
Cor Total	0.2251	19				

Table S4. Different statistical parameters are given in the table regarding zeta potential

Source	Sum of Squares	df	Mean Square	*F*-value	*p*-value	
Model	142.14	9	15.79	10.91	0.0004	significant
A-Surfactant	78.12	1	78.12	53.95	< 0.0001	
B-Amplitude	8.34	1	8.34	5.76	0.0373	
C-Drug	12.37	1	12.37	8.54	0.0152	
AB	0.8871	1	0.8871	0.6127	0.4519	
AC	1.35	1	1.35	0.9310	0.3574	
BC	3.21	1	3.21	2.22	0.1675	
A^2	5.88	1	5.88	4.06	0.0716	
B^2	23.39	1	23.39	16.16	0.0024	
C^2	4.84	1	4.84	3.34	0.0976	
Residual	14.48	10	1.45			
Lack of Fit	12.07	5	2.41	5.02	0.0506	not significant
Pure Error	2.40	5	0.4809			
Cor Total	156.62	19				

Table S5. Different statistical parameters are given in the table regarding drug content

Source	Sum of Squares	df	Mean Square	*F*-value	*p*-value	
Model	1595.35	9	177.26	66.34	< 0.0001	significant
A-Surfactant (X1)	86.49	1	86.49	32.37	0.0002	
B-Amplitude (X2)	80.86	1	80.86	30.26	0.0003	
C-Drug (X3)	1229.23	1	1229.23	460.03	< 0.0001	
AB	5.22	1	5.22	1.95	0.1926	
AC	0.6962	1	0.6962	0.2605	0.6208	
BC	5.22	1	5.22	1.95	0.1926	
A^2	18.18	1	18.18	6.80	0.0261	
B^2	18.01	1	18.01	6.74	0.0267	
C^2	171.48	1	171.48	64.18	< 0.0001	
Residual	26.72	10	2.67			
Lack of Fit	18.62	5	3.72	2.30	0.1912	not significant
Pure Error	8.10	5	1.62			
Cor Total	1622.07	19				

Table S6. In-vitro drug release kinetic models

Drug	Zero-order			First-order			Higuchi			Korsmeyer-Peppas		
	R^2	AIC	K_0	R^2	AIC	K_1	R^2	AIC	K_H	R^2	AIC	K_{kp} and (n)
KTZ	0.70	61.30	3.896	0.95	46.55	0.083	0.93	49.50	16.152	0.965	45.12	14.59 (0.54)
EUG	-10.4	64.71	9.272	0.42	59.52	0.065	0.83	49.58	14.43	0.964	39.15	21.41 (0.468)

References

[1] K. Bansal, D. Kakde, L. Purdie, D. Irvine, S. Howdle, G. Mantovani, C. Alexander, New Biomaterials from Renewable Resources - Amphiphilic Block Copolymers from δ-Decalactone, Polym Chem, 6 (2015).

[2] B. Alhasso, M.U. Ghori, B.R. Conway, Development of Nanoemulsions for Topical Application of Mupirocin, Pharmaceutics, 15 (2023).

[3] S. Chaturvedi, A. Garg, Development and optimization of nanoemulsion containing exemestane using box-behnken design, J Drug Deliv Sci Technol, 80 (2023) 104151.

[4] E.H. Endo, R.Y. Makimori, M.V.P. Companhoni, T. Ueda-Nakamura, C.V. Nakamura, B.P. Dias Filho, Ketoconazole-loaded poly-(lactic acid) nanoparticles: Characterization and improvement of antifungal efficacy in vitro against Candida and dermatophytes, J Mycol Med, 30 (2020) 101003.

[5] J. Chwiej, M. Szczerbowska-Boruchowska, M. Lankosz, S. Wojcik, G. Falkenberg, Z. Stegowski, Z. Setkowicz, Preparation of tissue samples for X-ray fluorescence microscopy, Spectrochim Acta Part B At Spectrosc, 60 (2005) 1531-1537.

[6] B. Tian, Q. Yan, J. Wang, C. Ding, S. Sai, Enhanced antifungal activity of voriconazole-loaded nanostructured lipid carriers against Candida albicans with a dimorphic switching model, Int J Nanomedicine, 12 (2017) 7131-7141.

[7] S.N. Chilamakuri, A. Kumar, A.G. Nath, A. Gupta, S. Selvaraju, S. Basrani, A. Jadhav, A. Gulbake, Development and In-Vitro Evaluation of Eugenol-Based Nanostructured Lipid Carriers for Effectual Topical Treatment Against C. albicans, J Pharm Sci, 113 (2023) 772-784.

[8] K.M. Hamad, N.N. Mahmoud, S. Al-Dabash, L.A. Al-Samad, M. Abdallah, A.G. Al-Bakri, Fluconazole conjugated-gold nanorods as an antifungal nanomedicine with low cytotoxicity against human dermal fibroblasts, RSC Adv, 10 (2020) 25889-25897.